# Supporting Information

## The construction of a 2D $MoS_2$-based binder-free electrode with honeycomb structure for promoted electrochemical performance

Shaokun Yin[a], Chao Li[a], Shicun Wang[b], Xiangkui Ren[a], Liang Zeng*[a], Lei Zhang*[a,c,d]

[a] *School of Chemical Engineering and Technology, Tianjin University, Tianjin, 300072, P. R. China*

[b] *China Nuclear Power Operation Technology Corporation, Ltd., Wuhan, Hubei, 430023, P. R. China*

[c] *Foshan (Southern China) Institute for New Materials, Guangdong 528000, P. R. China*

[d] *Center of Advanced Ceramic Materials and Devices, Yangtze Delta Region Institute of Tsinghua University, Zhejiang, 314006, P. R. China*

Emails of corresponding authors.

Lei Zhang, zll@tju.edu.cn

### Experimental section

*Synthesis of $MoS_2/Ni_3S_2$ on Ni foam, $Ni_3S_2$ on Ni foam and $MoS_2$ nanoparticles*

Ni foam was first cut into a 2×5 $cm^2$ rectangle and ultrasonically cleaned in acetone, 1 M HCl, deionized water, ethanol, then dried in a vacuum oven for 24 h and weighed. $MoS_2/Ni_3S_2$ was grown on Ni foam ($MoS_2/Ni_3S_2$/NF) by solvothermal and annealing method. Molybdenum powder (1 mmol) was dissolved into 1 mL hydrogen peroxide solution ($H_2O_2$, 30%) and the solution was dispersed into 50 mL deionized water and stirred for 2 h. Sulfur powder (2.2 mmol) was dissolved into 10 mL hydrazinium hydrate solution ($N_2H_4$, 50%) and stirred for 8h. The above solutions were mixed together and stirred for 2 h, then transferred into a 100 mL Teflon-lined stainless autoclave together with Ni foam, and heated at 180 ℃ for 6 h. The sample precursor was washed with deionized water for several times, and then dried at 60 ℃ for 12 h in a blast oven. Finally, the sample precursor was annealed at 300 ℃ for 2 h with the heating rate of 2 ℃/min in an atmosphere of 5% $H_2$/95% Ar. The same method was used to synthesize $Ni_3S_2$ on Ni foam ($Ni_3S_2$/NF) without adding Molybdenum powder, and $MoS_2$ nanoparticles ($MoS_2$/NPs) without adding Ni foam. The active materials loading is 2.03 mg $cm^{-2}$ for $MoS_2/Ni_3S_2$/NF and 6.245 mg $cm^{-2}$ for $Ni_3S_2$/NF.

*Material characterizations*

The crystal structures of samples were examined by an X-ray diffractometer (XRD, Bruker D8-Focus, Cu K$\alpha$ radiation, $\lambda$ = 1.54056 Å) generated at 40 kV and 40 mA in a range of 10~80° for 2θ values. The surface morphologies of samples were investigated by scanning electron microscopy (SEM, Hitachi S4800, Japan). At the same time, the element distribution was further analyzed with EDS elemental mapping. The microstructures were investigated by transmission electron microscopy (TEM, JEOL JEM3100, Japan) at 200 kV. X-ray photo-electron spectroscopy (XPS, Thermo Scientific, ESCALAB 250) with a monochromatic Al K$\alpha$ X-ray source was studied to analyze the oxidation states of the elements present in $MoS_2/Ni_3S_2$/NF.

*Electrochemical characterizations*

All the electrochemical examinations were investigated by CHI660E electrochemical workstation (Shanghai Chenhua, China). The three-electrode system was employed in 3 M KOH solution with 2×2 $cm^2$ platinum foil as the counter electrode, the Hg/HgO as the reference electrode, and the $MoS_2/Ni_3S_2$/NF 1×1 $cm^2$ squares as the working electrode. Cyclic voltammetry (CV) curves were investigated in a potential range of 0~0.7 V. Galvanostatic charge–discharge (GCD) was investigated in a potential range of 0~0.5 V. Electrochemical impedance spectroscopy (EIS) was measured in an AC voltage with 5 mV amplitude in a frequency range of 0.1~100 kHz. Cyclic performance was investigated using a battery testing system (Land, China) at 10 A $g^{-1}$. The same method was employed to test $Ni_3S_2$/NF and $MoS_2$/NPs (by mixing of 80 wt% $MoS_2$/NPs, 10 wt% carbon black, 10 wt% PTFE and pressing on 1×1 $cm^2$ Ni foam).

The strong redox CV peaks at various scan rates indicate that $MoS_2/Ni_3S_2$/NF exhibits obvious battery-type feature in KOH electrolyte with fast electrochemical kinetics. For battery-type electrode having a plateau during the charging/discharging, the capacity (mAh) should be applied. To compare with other research results, we also calculated the capacitance (Farad) here. The total charge, Q (C), specific capacity, $C_{sp\text{-}capacity}$ (mAh $g^{-1}$) and specific capacitance, $C_{sp\text{-}capacitance}$ (F $g^{-1}$) were calculated using the following equations:

$$Q = I \times \Delta t$$

$$C_{sp-capacity} = \frac{Q}{m \times 3.6} = \frac{I \times \Delta t}{m \times 3.6}$$

$$C_{SP-capacitance} = \frac{Q}{m \times \Delta V} = \frac{I \times \Delta t}{m \times \Delta V}$$

Where I, m, Δt and ΔV are the discharge current (A), mass of the active material (g), the discharge time (s) and potential window (V), respectively.

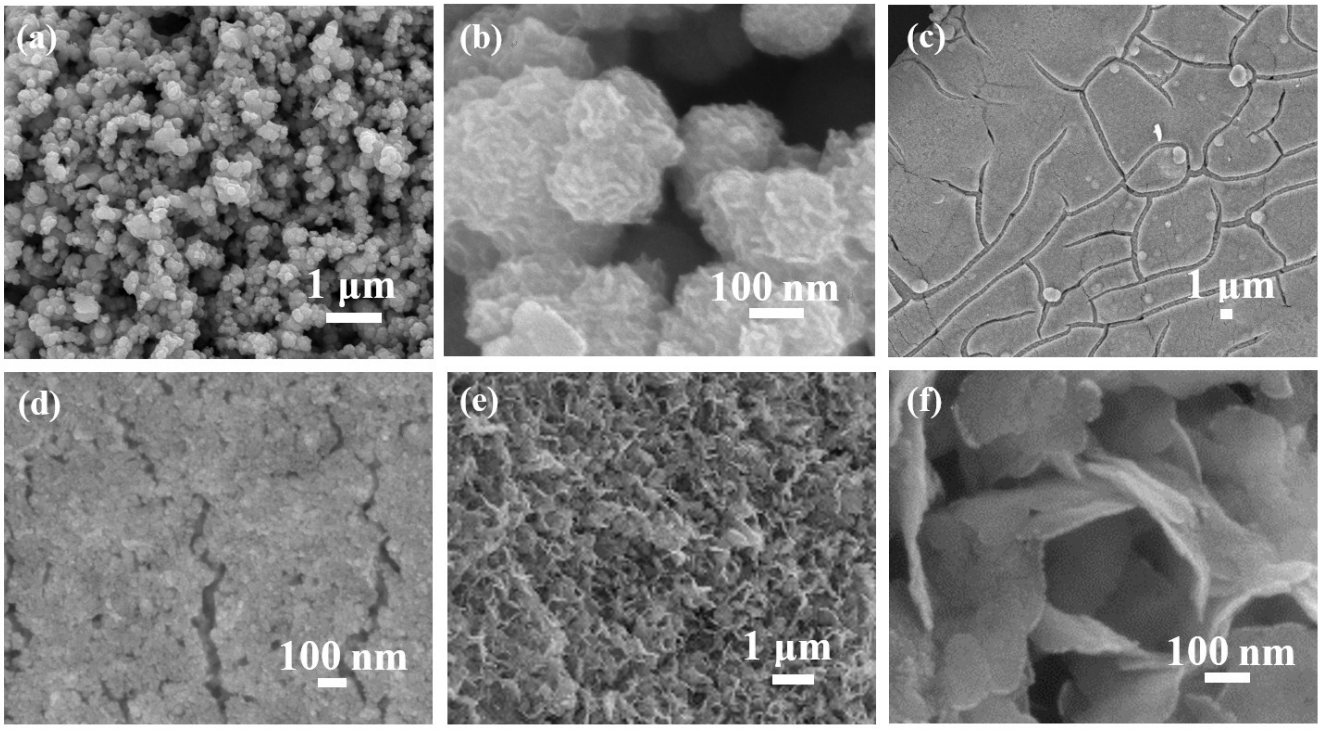


**Fig. S1.** SEM images of (a, b) $MoS_2$/NPs, (c, d) $Ni_3S_2$/NF, (e, f) $MoS_2/Ni_3S_2$/NF after stability test.

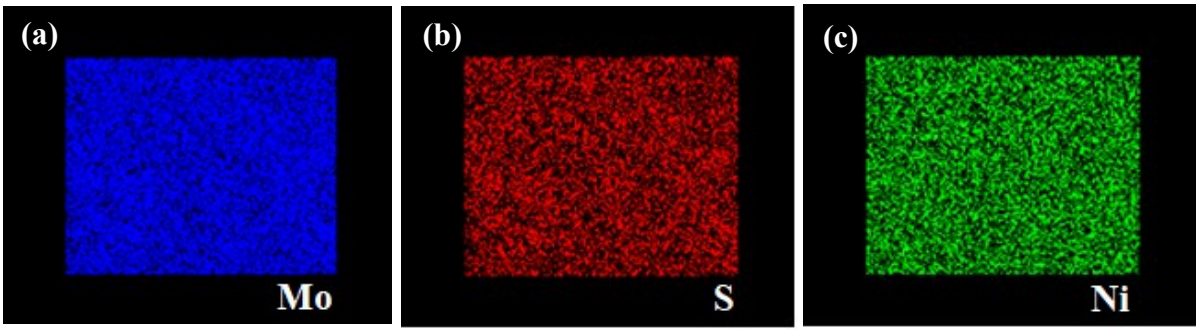


**Fig. S2.** EDS images of $MoS_2/Ni_3S_2$/NF.

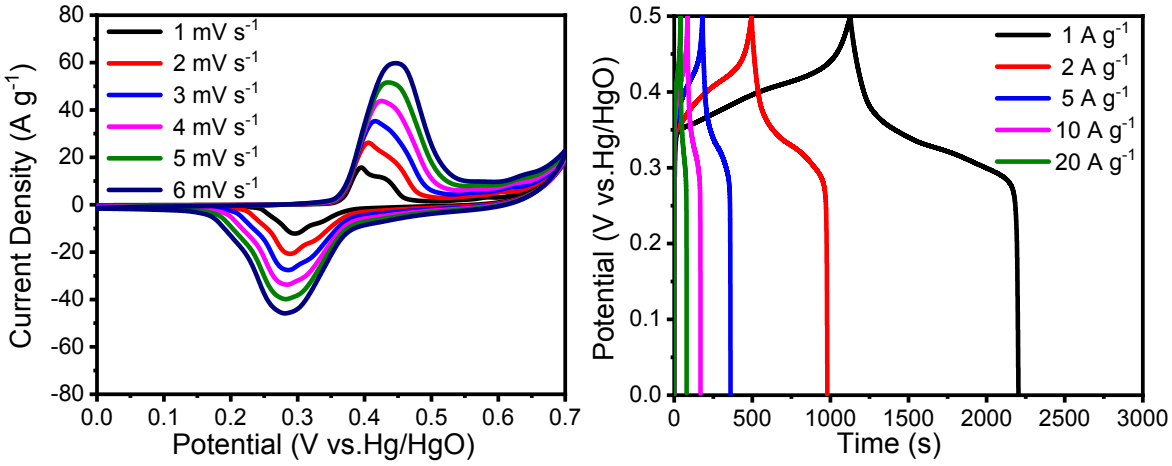


**Fig. S3.** Electrochemical characterizations of $MoS_2/Ni_3S_2$/NF (a) CV curves at 1-6 m V $s^{-1}$, (b) charge-discharge curves at 1-20 A $g^{-1}$.

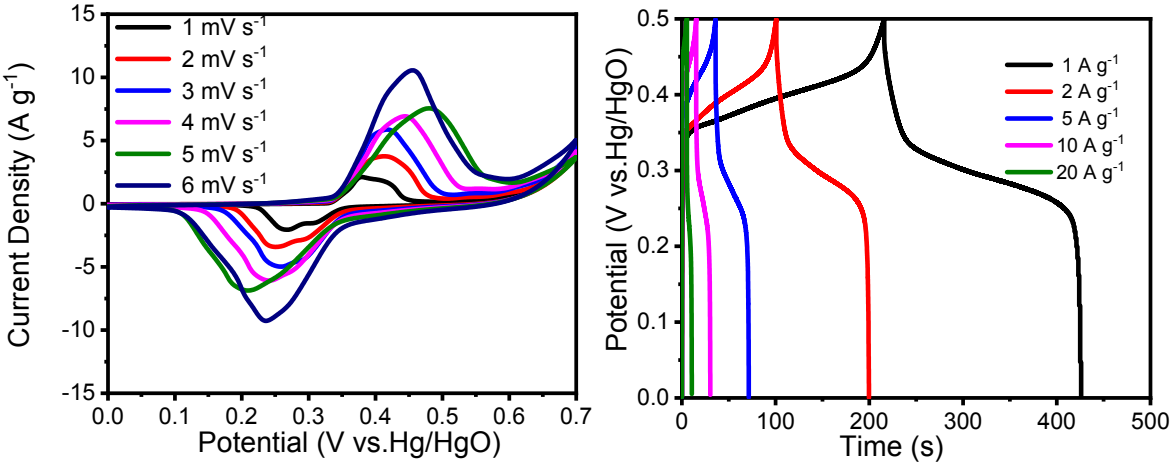


**Fig. S4.** Electrochemical characterizations of $Ni_3S_2$/NF (a) CV curves at 1-6 m V $s^{-1}$, (b) charge-discharge curves at 1-20 A $g^{-1}$.

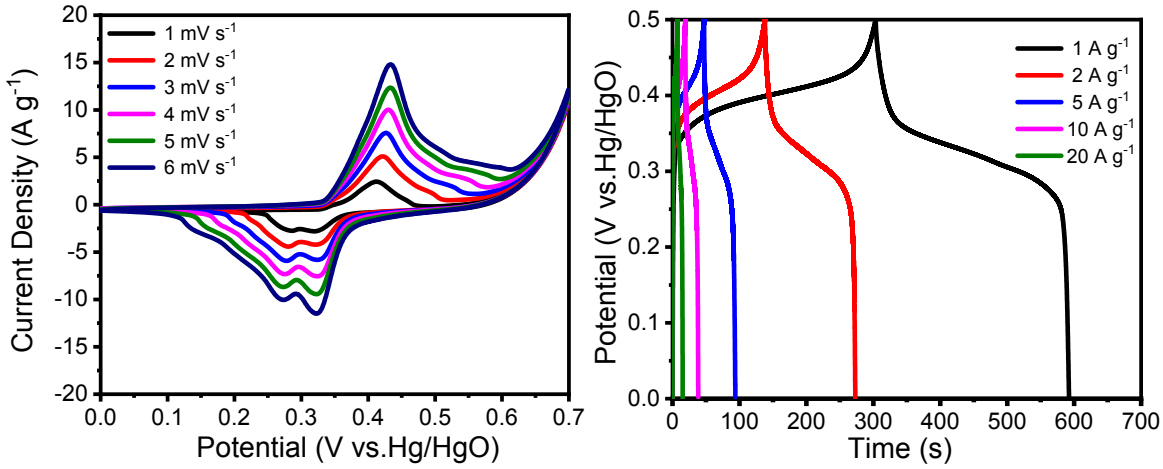


**Fig. S5.** Electrochemical characterizations of $MoS_2$/NPs (a) CV curves at 1-6 m V $s^{-1}$, (b) charge-discharge curves at 1-20 A $g^{-1}$.

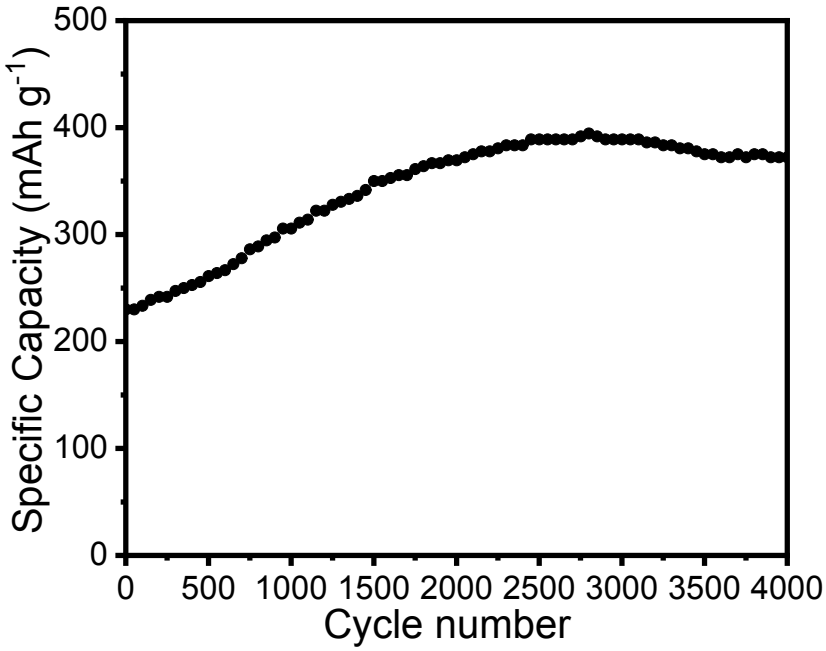


**Fig. S6.** Cycling stability of $MoS_2/Ni_3S_2$/NF at 10 A $g^{-1}$.

**Table S1** Electrochemical performance of different $MoS_2$-based electrode materials

| Electrode material | Electrolyte | Specific capacitance | Capacitance retention | Ref. |
|---|---|---|---|---|
| $MoS_2$@3D-Ni-foam | 1 M KOH | 3.4 F $cm^{-2}$ at 3 mA $cm^{-2}$ | 82% remained after 4500 cycles (at 3 mA $cm^{-2}$) | 1 |
| $MoS_2$/RGO/$Ni_3S_2$@NF | 2 M KOH | 1235.3 F $g^{-1}$ at 7 A $g^{-1}$ | 98.4% remained after 11000 cycles (at 7 A $g^{-1}$) | 2 |
| C@$MoS_2$/$Ni_3S_4$ | 2 M KOH | 951.3 F $g^{-1}$ at 2 A $g^{-1}$ | 80% remained after 10000 cycles (at 20 A $g^{-1}$) | 3 |
| $MoS_2$/$Co_3S_4$/$Ni_3S_4$ | 2 M KOH | 3.94 F $cm^{-2}$ at 5 mA $cm^{-2}$ | 91.8% remained after 5000 cycles (at 20 mA $cm^{-2}$) | 4 |
| $NiMoO_4$@$NiS_2$/$MoS_2$ | 6 M KOH | 970 F $g^{-1}$ at 5 A $g^{-1}$ | 60% remained after 5000 cycles (at 2 A $g^{-1}$) | 5 |
| $MoSe_2$@$MoS_2$ | 0.5 M $H_2SO_4$ | 1229.6 F $g^{-1}$ at 1 A $g^{-1}$ | 92.8% remained after 2000 cycles (at 1 A $g^{-1}$) | 6 |
| $MoS_2$/$Ni_3S_2$/NF | 3 M KOH | 1685.463 F $g^{-1}$ (234.10 mAh $g^{-1}$) at 10 A $g^{-1}$, 3.64 F $cm^{-2}$ at 10 mA $cm^{-2}$ | 160% remained after 4000 cycles (at 10 A $g^{-1}$) | This work |

## References

[1] D. K. Nandi, S. Sahoo, S. Sinha, S. Yeo, H. Kim, R. N. Bulakhe, J. Heo, J. J. Shim, S. H. Kim, Highly Uniform Atomic Layer-Deposited $MoS_2$@3D-Ni-Foam: A Novel Approach to Prepare an Electrode for Supercapacitors, ACS Applied Materials & Interfaces. 9 (2017) 40252-40264.

[2] C. Zhao, Y. Zhang, X. Qian, $MoS_2$/RGO/$Ni_3S_2$ Nanocomposite in-situ grown on Ni Foam substrate and its high electrochemical performance, Electrochimica Acta. 198 (2016) 135-143.

[3] S. Qin, T. Yao, X. Guo, Q. Chen, D. Liu, Q. Liu, Y. Li, J. Li, D. He, $MoS_2$/$Ni_3S_4$ composite nanosheets on interconnected carbon shells as an excellent supercapacitor electrode architecture for long term cycling at high current densities, Applied Surface Science. 440 (2018) 741-747.

[4] Y. Liu, S. Lin, Z. Xu, L. Li, Morphology evolution and electrochemical properties of hierarchical $MoS_2$/$Co_3S_4$/$Ni_3S_4$ nanosheet-on-nanorod arrays, Journal of Alloys and Compounds. 814 (2020) 152269.

[5] D. Chen, M. Lu, L. Li, D. Cai, J. Li, J. Cao, W. Han, Hierarchical core–shell structural $NiMoO_4$@$NiS_2$/$MoS_2$ nanowires fabricated via an in-situ sulfurization method for high performance asymmetric supercapacitors, Journal of Materials Chemistry A. 7 (2019) 21759-21765.

[6] S. Li, W. Zang, X. Liu, S. J. Pennycook, Z. Kou, C. Yang, C. Guan, J. Wang, Heterojunction engineering of $MoSe_2$/$MoS_2$ with electronic modulation towards synergetic hydrogen evolution reaction and supercapacitance performance, Chemical Engineering Journal. 359 (2019) 1419-1426.